Biosynthesis of titanium oxide nanoparticles using star anise and evaluation of their inhibitory activity against some food poisoning microbes contaminating meat

Sarah Samir Daoud 1, Manal Saleh Mahdi 2
1-2Department of Food Sciences, College of Agriculture, Tikrit University, Tikrit, Iraq
1 sd230010pag@st.tu.edu.iq
2manalsaleh@tu.edu.iq

Abstract
The study was conducted at the Food Science Department and Central Laboratories, College of Agriculture, Tikrit University, from February 15 to August 22, 2025. The aim was the biosynthesis of titanium oxide nanoparticles (TiO_2 -NPs) using star anise (Illicium verum) and the evaluation of their inhibitory activity against foodborne pathogens isolated from meat, including Staphylococcus aureus, E. coli, Pseudomonas aeruginosa, and Salmonella, identified using standard tests. UV-Visible spectroscopy of the aqueous star anise extract treated with TiO_2 -NPs showed an absorption range between 280–800 nm with a sharp peak at 280–300 nm (1.9 absorbance units), confirming strong UV absorption typical of nanostructured TiO_2 . FTIR analysis revealed characteristic peaks indicating chemical interactions during biosynthesis, while XRD analysis confirmed crystalline nanoparticle formation. The aqueous star anise extract demonstrated variable antibacterial activity. It inhibited Salmonella and E. coli effectively but showed no effect against Staphylococcus aureus and Pseudomonas aeruginosa. Inhibition zones for Salmonella at 125, 250, 500, and 1000 µg/ml were 1.8, 2.0, 3.8, and 3.8 cm, respectively. Results highlighted the strong antimicrobial efficiency of the plant–nanoparticle combination, though only limited inhibitory effects were observed against three bacterial strains.
Key words: Titanium nanoparticles, star anise, food poisoning, bacteria, meat

Introduction

Bacterial diseases caused by microorganisms, especially bacteria, are among the most widespread types of infections worldwide. Bacteria are ancient and abundant organisms, with fossilized forms dating back nearly 3 billion years. Many species of bacteria can cause disease in humans and other organisms due to their chemical and genetic characteristics [1]. One of the most pressing challenges facing the food production industry is the production of healthy food products without artificial preservatives, given that synthetic antibacterial agents and chemical additives can have serious adverse effects on people's quality of life. Essential oils extracted from plant sources have received significant attention due to their potential health benefits. Essential oils consist of complex components that include many distinct chemicals isolated using various methods. These diverse chemicals have demonstrated significant biological functions, such as antioxidant and antibacterial activity, through a variety of mechanisms [2]. Contamination of food with pollutants and heavy metals can lead to serious illnesses in the food consumed by humans [3]. To address this, research is focusing on alternatives such as metallic nanomaterials,

ISSN 2072-3857

which hold promise as novel antimicrobials. Nanoparticles exhibit unique physical and chemical properties compared to their bulk forms, enabling wide-ranging applications from electronics to medicine. Elements considered safe in bulk can exhibit severe toxicity at the nanoscale due to their increased surface area and reactivity [4]. Star anise (Illicium verum), a spice from the Schisandraceae family, is widely used in the pharmaceutical and food industries. It contains essential oils with antibacterial, antifungal, anti-inflammatory, and antioxidant effects. Its main component, trans-anethole, is widely used in foods, perfumes, and pharmaceuticals, exhibiting antioxidant, anti-inflammatory, and anti-obesity properties [5]. Star anise (Illicium verum) also contains phenolic and flavonoid compounds, which give it a high antioxidant capacity by inhibiting free radicals and increasing the reducing capacity. It also contains trans-anethole, a compound with strong antimicrobial activity, having demonstrated activity against bacteria (such as Escherichia coli and Staphylococcus aureus) and fungi (such as Candida albicans). Therefore, star anise is a promising plant for use in the food and pharmaceutical fields as a natural alternative to synthetic antibiotics [6]. Among nanomaterials, titanium dioxide nanoparticles (TiO_2 NPs) are widely used in consumer products, agriculture, and energy. However, their extensive use raises environmental and health concerns. Understanding its toxicity is crucial for safe applications. The toxicity of titanium dioxide nanoparticles in microorganisms, algae, plants, invertebrates, and vertebrates mainly includes: (1) formation of reactive oxygen species under light exposure, (2) cell wall damage and lipid peroxidation resulting from electrostatic interactions with large surface area molecules, and (3) cytoplasmic leakage and dissociation of organelles and biomolecules after membrane damage [7]. Meat is a staple food with high nutritional value, providing complete proteins rich in essential amino acids for tissue building and repair. It is also an important source of highly absorbable heme iron, zinc, selenium, and water-soluble vitamins, such as B vitamins, especially vitamin B12, which is essential for blood formation and nervous system function. Meat contains varying amounts of fat, which provides energy and essential fatty acids and aids in the absorption of fat-soluble vitamins. However, meat is highly perishable due to its high water and protein content, making it an ideal medium for the growth of microorganisms such as bacteria and fungi. Microbial contamination during slaughter or handling, high temperatures, and improper storage accelerate microbial and enzymatic spoilage, resulting in discoloration, off-odors, and the formation of a slimy surface layer. Therefore, good hygiene practices and maintaining a cold chain (refrigeration and freezing) are essential to prolong the shelf life and maintain the nutritional quality of meat [8 .[

Materials and Methods

Sterilization and Media Preparation

Glassware was sterilized by dry heat in an oven at 180 °C for 2 h, while inoculating tools were flame-sterilized using a Bunsen burner. All culture media and solutions requiring moist sterilization were autoclaved at 121 °C, 15 psi for 15 min [9]. Culture media were prepared according to manufacturer instructions, dissolved in distilled water by boiling, sterilized at 121 °C for 15 min, then poured into sterile Petri dishes at 50 °C.

ISSN 2072-3857

Sterility was confirmed by incubation at 30 °C for 24 h [10.[

Reagents & Solutions

Reagents were prepared following standard protocols:

- Gram's stain solutions [11.[
- Normal saline: 8.5 g NaCl/L distilled water, pH 7.2 [12.[
- MacFarland Standard (0.5 tube): prepared from $BaCl_2$ and H_2SO_4 solutions, giving ≈1.5×10^8 cells/ml [13.[

Sample Collection

Random fresh meat samples were collected from Tikrit markets in sterile containers, cooled, and transported to the lab for bacterial isolation.

Microbial Isolation

Ten grams of meat were homogenized in 90 ml saline, serially diluted, and plated (0.1 ml) on culture media using an L-shaped spreader. Plates were incubated at 37 °C for 24 h. Colonies were purified by streaking on selective media and identified via morphological, microscopic, and biochemical tests.

Preservation of Isolates

Bacterial isolates were maintained on nutrient agar slants at 4 °C and sub-cultured monthly to ensure viability [14.[

Nanoparticle Characterization

- UV-Vis Spectroscopy (200–800 nm) for optical properties [15.[
- FTIR (4000–600 cm^{-1}) for functional group analysis [16.[
- XRD for crystal structure and particle size [17.[
- SEM for morphology and size at 12.5–15 kV [18.[

Nanoparticle Preparation

TiO_2 -star anise nanocomposite was synthesized [19] by mixing 1 g star anise with 1 g TiO_2 oxide in 50 ml deionized water, stirred for 24 h, incubated at 40 °C for 18 h, centrifuged (3000 rpm, 20 min), washed, dried at 50 °C, ground, and stored. Serial concentrations (125–1000 µg/ml) were prepared for testing.

Antibacterial Assay

The inhibitory effect of star anise extract and TiO_2 -star anise nanocomposite was tested against E. coli, Salmonella, Staphylococcus aureus, and Pseudomonas using agar well diffusion (MHA medium). Wells were filled with concentrations of 125–1000 µg/ml. Plates were incubated at 37 °C for 24 h, and inhibition zones measured [20.[

Statistical Analysis

The experiment followed a Complete Randomized Design (CRD). Data were analyzed using the General Linear Model (GLM) procedure in [21]. Significant differences among means were determined using Duncan's test at $p \leq 0.05$ [22 .[

Results and discussion

Diagnosis of nanocomposites:

-1Scanning Electron Microscopy

When scanning electron microscopy (SEM) was used to examine the morphology of nanoparticles biosynthesized using star anise extract, the results (Figure 1) showed that titanium dioxide nanoparticles were irregular in shape, with diameters ranging from 54.84 to 252.5 nm. These results indicate that the mineral type strongly influences particle size and morphology, reflecting the role of plant

ISSN 2072-3857

bioactive compounds in nanoparticle formation. These results are consistent with [23], who reported that plant-derived nanoparticles typically range from 25 to 130 nm, depending on the mineral and phytochemicals used. They also highlighted the role of phenolics and flavonoids in reducing ions and stabilizing nanoparticles, contributing to their biomedical potential. Overall, SEM analysis confirmed that titanium dioxide nanoparticles were smaller and more regular in size. This morphological difference directly affects the physical, chemical, and functional properties of nanoparticles, highlighting the importance of selecting the appropriate metal and extractant for specific applications .

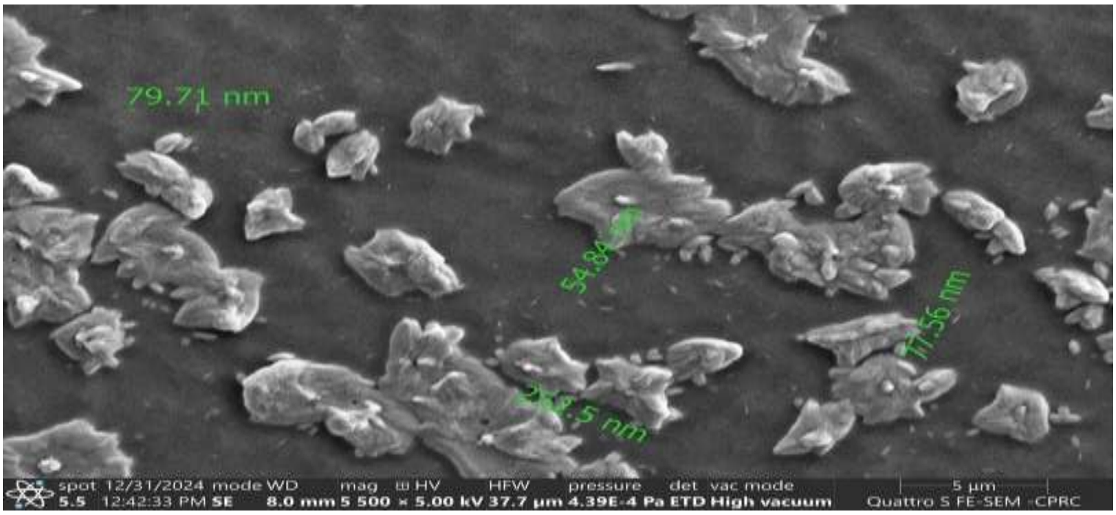

Figure (1) shows the size and shape of the star anise extract particles with the addition of titanium nanoparticles.

-2UV-Vis Spectroscopy

UV-Vis spectroscopy analysis of the aqueous star anise extract treated with titanium oxide nanoparticles revealed distinct absorption patterns (Figure 2), confirming the nanoparticle formation and their photoresponse. The titanium oxide nanoparticles (Figure 2) exhibited absorption between 280 and 800 nm, with a stronger peak (approximately 1.9 units) at 280–300 nm, reflecting higher UV absorption efficiency. These results are consistent with [24], who reported that titanium oxide nanoparticles typically exhibit strong UV absorption peaks at wavelengths between 280 and 320 nm due to electron transitions from the valence band to the conduction band. This spectral behavior is a hallmark of semiconductor nanoparticles and is associated with quantum confinement effects and an enhanced surface-to-volume ratio, supporting their use in antibacterial, photocatalysis, and biomedical applications. The difference in peak intensity (1.5 vs. 1.9) is attributed to differences in crystal structure and surface properties. Titanium oxide, with its unique electron configuration, enables more efficient electron transitions in the UV range, making it superior in photocatalysis and optoelectronic devices [25 .[

ISSN 2072-3857

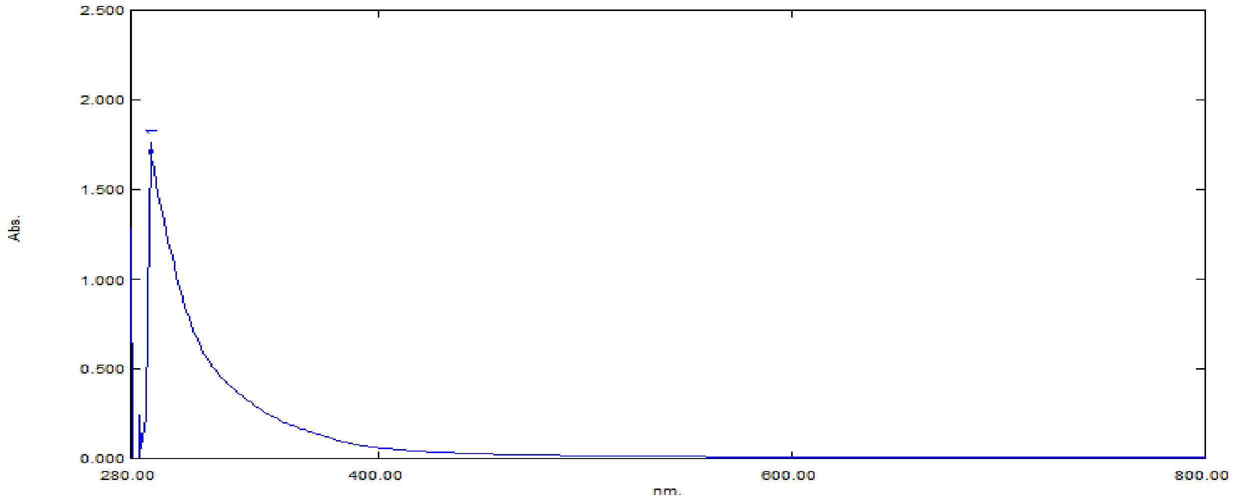

Figure (2) UV spectrum of star anise extract with the addition of titanium oxide nanoparticles.

.3Diagnosis using FTIR spectroscopy: FTIR analysis of the aqueous star anise extract treated with titanium oxide nanoparticles revealed several characteristic peaks reflecting chemical reactions during biosynthesis. FTIR is a key tool for identifying functional groups attached to nanoparticle surfaces, confirming their formation and stabilization by phytochemicals. For TiO_2 -NPs (Figure 3), a clear absorption at 600–500 cm^{-1} was attributed to Ti–O–Ti vibrations, confirming the formation of nanoparticles, while a broad band at 3400–3200 cm^{-1} indicated hydroxyl groups. These results are consistent with [26], who indicated that the absorption bands at 500–700 cm^{-1} are typical of Zn–O and Ti–O bonds, while the broad peaks at 3200–3400 cm^{-1} reflect OH^- groups of water or phenolic compounds. [27] The bands at 1700–1600 cm^{9} were associated with carboxyl or carbonyl groups involved in the reduction and stabilization of nanoparticles, while the bands at 2920–2850 cm^{9} indicate organic interactions with the nanoparticle surfaces. Studies [28] have confirmed that phytochemicals—especially phenolics and flavonoids—act simultaneously as reducing and capping agents, forming stable organic layers around nanoparticles and enhancing their functional performance. Overall, Fourier transform infrared spectra confirmed that star anise extract not only reduces metal ions but also provides stabilizing biomolecules, preventing agglomeration and supporting the efficient green synthesis of bioactive nanoparticles

.

ISSN 2072-3857

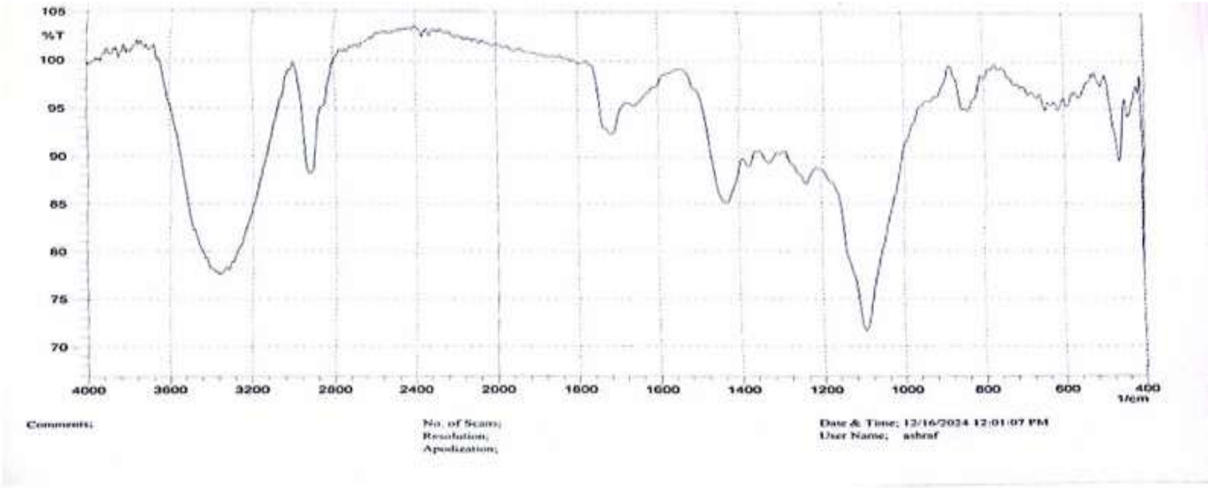

Figure (3) FTIR spectrum of star anise extract with the addition of titanium oxide nanoparticles.

-4X-ray Diffraction Microscope

X-ray diffraction (XRD) analysis of titanium oxide nanoparticles extracted from star anise revealed distinct crystalline patterns, confirming the successful formation of nanoparticles (Figure 4). X-ray diffraction is an essential tool for determining crystal phase, purity, and crystal size. For titanium oxide nanoparticles (Figure 4), multiple sharp peaks were observed at angles of 25°, 27.5°, and ~30.8° (2θ), reflecting well-defined crystal planes characteristic of the anatase phase. The peak intensities (80–90 counts) and narrow widths indicated larger and more organized crystals. This difference is attributed to the interaction between star anise phytochemicals and metal ions, which affects crystallization and crystallization rates. These results are consistent with [29], who reported that titanium oxide had sharp peaks typical of high-purity anatase or rutile phases. Similarly, [30] indicated that broad peaks represent small nanocrystals, while sharp peaks indicate larger, more organized crystals. In conclusion, star anise extract effectively facilitated the biosynthesis of pure titanium oxide nanoparticles, while titanium dioxide formed larger, more organized crystals—highlighting their potential in various biomedical and industrial applications .

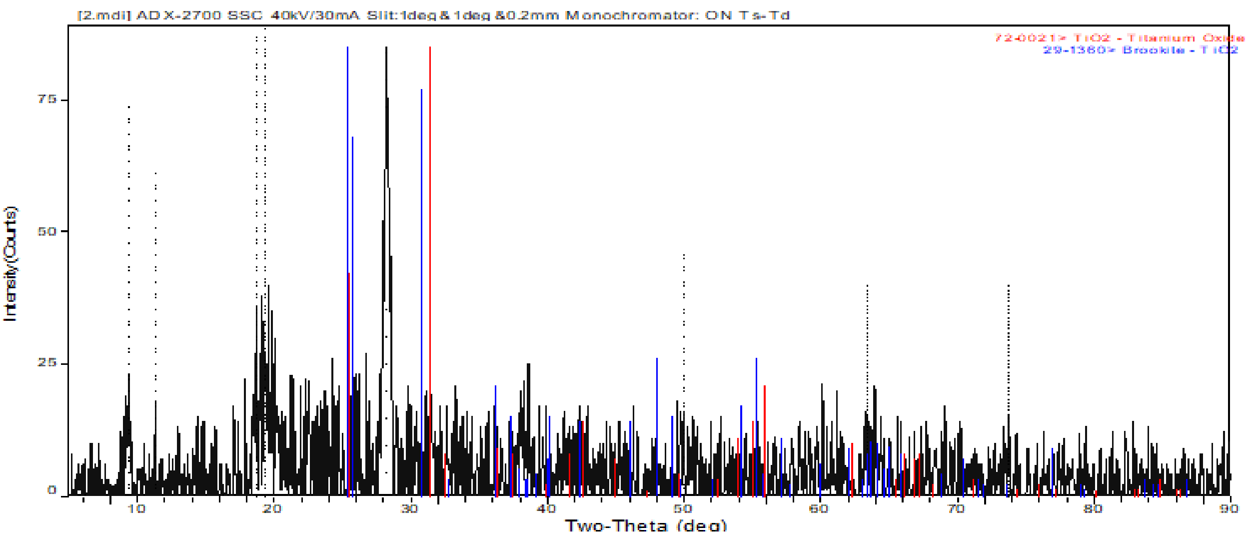

Figure (4) X-ray diffraction of star anise extract with the addition of titanium oxide nanoparticles.

The inhibitory effect of star anise extract enriched with titanium oxide nanoparticles on some microorganisms isolated from meat:

The aqueous extract of star anise combined with TiO_2 nanoparticles was tested for antibacterial activity against meat-isolated bacteria Table (1). Results showed limited inhibitory effects against three bacterial strains, while Staphylococcus aureus exhibited complete resistance. The activity was assessed by measuring inhibition zones at concentrations of 125, 250, 500, and 1000 µg/mL. For Salmonella spp., inhibition zones increased slightly with concentration (1.0, 2.0, 2.1, 2.3 cm), indicating a moderate, dose-dependent response. This effect is linked to reactive oxygen species (ROS) generated by photoactivated TiO_2 , which damage bacterial membranes and cellular functions, consistent with [31]. For E. coli, inhibition zones fluctuated (2.0, 1.5, 2.2, 3.1 cm), showing cumulative effects at higher concentrations but reduced activity at 250 µg/mL. According to [32], TiO_2 activity against E. coli strongly depends on nanoparticle stability and dispersion in aqueous media; poor distribution or aggregation may explain the inconsistent inhibition observed. Pseudomonas aeruginosa, known for high antibiotic resistance, showed gradual inhibition (1.0, 1.6, 2.5, 2.8 cm) with increasing concentration. This reflects TiO_2 's ability to penetrate cell membranes, disrupt permeability and protein functions, and inhibit growth, in agreement with [33]. By contrast, S. aureus showed no inhibition at all concentrations (0.0 cm), confirming the limited efficacy of TiO_2 against Gram-positive bacteria due to their thick cell walls. These findings align with [34], who reported weaker TiO_2 effects on Gram-positive strains .

Table (1) Inhibitory activity of star anise extract enriched with titanium oxide nanoparticles against some types of bacteria isolated from meat.

N. O	Bacteria	Inhibition zone (cm)			
		Nano Titanium Oxide Enriched Hydrolyzed Star Anise (µg/mm)			
		125 gµ\ml	250 gµ\ml	500 gµ\ml	1000 gµ \ml
1	Salmonella	1.0 a	2.0 a	2.1 a	2.3 a
2	E. coli	2.0 b	1.5 b	2.2 a	3.1 a
3	Staphylococcus aureus	0.0 a	0.0 a	0.0 a	0.0 a
4	Pseudomonas aeruginosa	1.0 b	1.6 b	2.5 a	2.8 a

Different letters in a row indicate significant differences between means at the 0.05 probability level.

Inhibitory activity of titanium oxide nanoparticles against some types of bacteria isolated from meat:

Table (2) illustrates the inhibitory activity of TiO_2 nanoparticles against meat-isolated bacteria at concentrations of 125, 250, 500, and 1000 µg/mL. The results showed variable bacterial responses, reflecting differences in cell sensitivity to nanoparticles. For Salmonella spp., inhibition zones increased progressively (1.0, 2.0, 3.7, 3.7 cm), with clear dose-dependent activity up to 500 µg/mL, after which the effect plateaued. This agrees with [35], who reported that TiO_2 generates reactive oxygen species (ROS) causing bacterial cell damage, especially in plant-based nanocomposites. E. coli exhibited relatively stable inhibition (2.2–3.0 cm) across concentrations, indicating moderate but consistent sensitivity. According to [35], TiO_2 shows antibacterial activity against Gram-negative species like E. coli, though its effectiveness depends on nanoparticle stability and dispersion. By contrast, Staphylococcus aureus showed complete resistance (0.0 cm at all concentrations). Overall, TiO_2 nanoparticles demonstrated partial antibacterial.

Table (2) Inhibitory activity of titanium oxide nanoparticles against some types of bacteria isolated from meat.

N. O	Bacteria	Inhibition zone (cm)			
		Titanium oxide particle concentration (µg/mm) TiO_2			
		125 gµ \ml	250 gµ \ml	500 gµ\ml	1000 gµ \ml
1	Salmonella	1.0 b	2.0 b	3.7 a	a 3.7
2	E. coli	2.2 a	2.8 a	2.8 a	3.0 a
3	Staphylococcus aureus	0.0 a	0.0 a	0.0 a	0.0 a
4	Pseudomonas aeruginosa	0.0 a	1.5 a	2.0 a	2.0 a

Different letters in a row indicate significant differences between means at the 0.05 probability level.

ISSN 2072-3857

Conclusion

We conclude that star anise enhanced with titanium oxide nanoparticles demonstrated limited inhibitory activity against three bacteria isolated from meat. The three bacteria exhibited varying inhibitory responses, confirming the high efficiency of the nano-plant mixture in inhibiting the growth of microorganisms.

References

[1]Murray, P. R., Rosenthal, K. S., & Pfaller, M. A. (2020). Medical Microbiology E-Book. Elsevier Health Sciences.

[2]Fadhil, Y. (2023). Usage of essential oils of natural herbs as food preservatives. Tikrit Journal for Agricultural Sciences, 23(1), 67-74.

[3]Albashr, T. K. M., Al-Magsoosi, S., Rashid, N. J., & Khidhir, Z. K. (2024). Determine the levels of heavy metal residues in different parts of chicken in the Tikrit and Beji cities of Iraq. Tikrit Journal for Agricultural Sciences, 24(2), 311-327.

[4]Emami-Karvani, Z. and Chehrazi, P. (2011). Antibacterial activity of ZnO nanoparticle on gram positive and gram-negative bacteria. African Journal of Microbiology Research. 5(12): 1368-1373 p.

[5]Patra, J.K.; Das, G.; Bose, S.; Banerjee, S.; Vishnuprasad, C.N.; del Pilar Rodriguez-Torres, M.; Shin, H.S. (2020) Star anise (Illicium verum): Chemical compounds, antiviral properties, and clinical relevance. Phyther, 34, 1248–1267.

[6]Wang, G. W., Hu, W. T., Huang, B. K., & Qin, L. P. (2011). Illicium verum: A review on its botany, traditional use, chemistry and pharmacology. Journal of Ethnopharmacology, 136(1), 10–20.

[7]Hou, J., Wang, L., Wang, C., Zhang, S., Liu, H., Li, S., & Wang, X. (2019). Toxicity and mechanisms of action of titanium dioxide nanoparticles in living organisms. Journal of environmental sciences, 75, 40-53.

[8]Ding, W., Lu, Y., Xu, B., Chen, P., Li, A., Jian, F., ... & Huang, S. (2024). Meat of sheep: insights into mutton evaluation, nutritive value, influential factors, and interventions. Agriculture, 14(7), 1060.

[9]Al-Maamouri, Abdul Nabi Juwaid and Al-Maamouri, Ishraq Abdul Amir. (2016). Diagnostic Migration Revival. First Edition, Safa Publishing and Distribution House - Amman.

[10]Atlas, R. M. (2004). Handbook of microbiological media. CRC press.

[11]Winn, W. C. (2006). Koneman's color atlas and textbook of diagnostic microbiology. Lippincott williams & wilkins.

[12]Atlas, R. M., Brown, A. E., and Parks, L. C. (1995). Laboratory manual of experimental microbiology. Mosby.

[13]AL-Ani, R. T. (2011). Studying the effect of organic solvent extracts for Euphorbia prostrata against bacteria Staphylococcus aureus and Pseudomonas aeruginosa in vitro. ANBAR JOURNAL OF AGRICULTURAL SCIENCES, 9(2.(

[14]Vandepitte, J., K. Engback, P. Piot and C. Henck. (1999). Basic Laboratory Procedures in Clinical Bacteriology, W.H.O.

[15]Duan, Y., Han, L., Zhang, J., Asahina, S., Huang, Z., Shi, L., ... & Che, S. (2015).

ISSN 2072-3857

Optically active nanostructured ZnO films. Angewandte Chemie International Edition, 54(50), 15170-15175.

[16]Ezealisiji, K. M., Siwe-Noundou, X., Maduelosi, B., Nwachukwu, N., & Krause, R. W. M. (2019). Green synthesis of zinc oxide nanoparticles using Solanum torvum (L) leaf extract and evaluation of the toxicological profile of the ZnO nanoparticles–hydrogel composite in Wistar albino rats. International Nano Letters, 9(2), 99-107.

[17]Zhang L, Jiang Y, Ding Y, Povey M, York D (2007) Investigation into the antibacterial behaviour of suspensions of ZnO nanoparticles (ZnO nanofluids). J Nanopart Res 9:479–489.

[18]Caroling, G., Tiwari, S. K., Ranjitham, A. M., & Suja, R. (2013). Biosynthesis of silver nanoparticles using aqueous broccoli extract-characterization and study of antimicrobial, cytotoxic effects. Asian J Pharm Clin Res, 6(4), 165-172.

[19]Bashi, A. M., Zobir, M., Zainal, Z., & Tichit, D. (2013). Journal of Solid-State Chemistry Synthesis and controlled release properties of 2, 4 dichlorophenoxy acetate – zinc layered hydroxide nanohybrid. Journal of Solid-State Chemistry, 203, 19–24.

[20]Bauer, A. W. (1996). Antibiotic susceptibility testing by a standardized single disc method. Am. J. of Clinc. Path., 45, 149-158.

[21]SAS (2001). Version, Statistical Analysis System, SAS Institute Inc., Cary, NC. 27512 – 8000, U.S.A.

[22]Duncan, D. B. (1955). Multiple range and multiple F tests. biometrics, 11(1), 1-42.

[23]Karmous, I., Pandey, A., Haj, K. B., & Chaoui, A. (2020). Efficiency of the green synthesized nanoparticles as new tools in cancer therapy: insights on plant-based bioengineered nanoparticles, biophysical properties, and anticancer roles. Biological trace element research, 196, 330-342.

[24]Pathania, S., Hmar, J. J. L., Verma, B., Majumder, T., Kumar, V., & Chinnamuthu, P. (2022). Titanium dioxide (TiO2) sensitized zinc oxide (ZnO)/conducting polymer nanocomposites for improving performance of hybrid flexible solar cells. Journal of Electronic Materials, 51(10), 5986-6001.

[25]Li, Z., Li, Z., Zuo, C., & Fang, X. (2022). Application of nanostructured TiO2 in UV photodetectors: a review. Advanced Materials, 34(28), 2109083.

[26]Pasieczna-Patkowska, S., Cichy, M., & Flieger, J. (2025). Application of Fourier Transform Infrared (FTIR) Spectroscopy in Characterization of Green Synthesized Nanoparticles. Molecules, 30(3), 684.

[27]SALIMI NADEM, P. (2023). Engineering of waste Biomass-based active materials for application in current Lithium-ion Batteries and Beyond.

[28]Ong, G., Kasi, R., & Subramaniam, R. (2021). A review on plant extracts as natural additives in coating applications. Progress in Organic Coatings, 151, 106091.

[29]Abd El Hamid, D. K., Desouky, E. M., AbdEllatif, S., Abed, N., & Mahfouz, A. Y. (2024). Green Synthesis and characterization of Titanium Dioxide nanoparticles by Aspergillus Niger DS22 and its potential application in Medical Fields. Egyptian Journal of Botany, 64(2), 629-653.

[30]Dan, K., Satpati, B., & Datta, A. (2024). Synergistically controlled in situ growth of silver nanoparticles leading to organization of anisotropic liquid crystalline medium. Liquid Crystals, 1-14.

[31]Yong, S. S., Lee, J. I., & Kang, D. H. (2023). TiO2-based photocatalyst Generated Reactive Oxygen Species cause cell membrane disruption of Staphylococcus

aureus and Escherichia coli O157: H7. Food Microbiology, 109, 104119.

[32]Imad Abd-AlAziz, S., Thalij, K. M., & Zakari, M. G. (2023). Inhibitory Susceptibility of Synthetic Selenium Nanoparticles and some Conjugate Nutritional Compounds in Inhibition of some Bacterial Isolates Causing Food Poisoning. Tikrit Journal for Agricultural Sciences, 23(4), 26-34.

[33]Ramadan, T., Sayed, S. A., Abd-Elaal, A. K., & Amro, A. (2022). The combined effect of water deficit stress and TiO2 nanoparticles on cell membrane and antioxidant enzymes in Helianthus annuus L. Physiology and Molecular Biology of Plants, 28(2), 391-409.

[34]Sayadi, M., Mojaddar Langroodi, A., Amiri, S., & Radi, M. (2022). Effect of nanocomposite alginate- based film incorporated with cumin essential oil and TiO2 nanoparticles on chemical, microbial, and sensory properties of fresh meat/beef. Food Science & Nutrition, 10(5), 1401-1413.

[35]Abd El-Aziz, M. A., Ibrahim, H. M., El-Roos, N. A., Anis, B., & Elsabagh, R. (2020). Antibacterial efficacy of zinc oxide and titanium dioxide nanoparticles against Escherichia coli in minced meat. World's Veterinary Journal, (3), 267-275

ISSN 2072-3857